Four-electron reduction of dioxygen by a multicopper oxidase, CueO, and roles of Asp112 and Glu506 located adjacent to the trinuclear copper center

doi: 10.1074/jbc.M808468200

Four-Electron Reduction of Dioxygen by a Multicopper Oxidase, CueO, and Roles of Asp112 and Glu506 Located Adjacent to the Trinuclear Copper Center

Kunishige Kataoka[1], Ryosuke Sugiyama[1], Shun Hirota[2], Megumi Inoue[1], Kanae Urata[1], Yoichi Minagawa[1], Daisuke Seo[1], and Takeshi Sakurai[1,*]

From the Graduate School of Natural Science and Technology, Kanazawa University, Kakuma, Kanazawa 920-1192, Japan[1]

Graduate School of Materials Science, Nara Institute of Science and Technology, Ikoma, Nara 630-0192, Japan[2]

Running title: Four-electron reduction of dioxygen by CueO

Address correspondence to: Takeshi Sakurai. Graduate School of Natural Science and Technology, Kanazawa University, Kakuma, Kanazawa, 920-1192, Japan. Fax: +81-76-264-5742: E-mail: ts0513@kenroku.kanazawa-u.ac.jp

The mechanism of the four-electron reduction of dioxygen by a multicopper oxidase, CueO was studied based on reactions of single and double mutants with Cys500, a type I Cu ligand, and the non-coordinating Asp112 and Glu506, which form hydrogen-bonds with the trinuclear Cu center directly and indirectly via a water molecule. The reaction of Cys500Ser containing a vacant type I Cu center produced the intermediate I in an EPR-silent peroxide-bound form. The formation of the intermediate I from Cys500Ser/Asp112Asn was restricted due to a reduction in the affinity of the trinuclear Cu center for dioxygen. The state of the intermediate I was realized to be the resting form of Cys500Ser/Glu506Gln and Cys500Ser of the truncated mutant Δα5-7CueO, in which the fifty amino acids covering the substrate-binding site were removed. Reactions of the recombinant CueO and Glu506Gln afforded the intermediate II, a fully oxidized form different from the resting one, with a very broad EPR signal, g < 2, detectable only at cryogenic temperatures and unsaturated with high power microwaves. The lifetime of the intermediate II was prolonged by the mutation at Glu506 involved in the donation of protons. The structure of the intermediates I and II and the mechanism of the four-electron reduction of dioxygen driven by Asp112 and Glu506 are discussed.

CueO is a multicopper oxidase involved in a copper efflux system of *Escherichia coli* (1-3). Differing from other multicopper oxidases such as laccase and ascorbate oxidase (4), CueO exhibits strong activity toward cuprous ion, but does not show activity toward most organic substrates such as 2,6-dimethoxyphenol, catechol, and guaiacol except considerably low levels toward 2,2'-azino-bis(3-ethylbenzothiazoline-6-sulfonic acid) (ABTS) and *p*-phenylenediamine. This substrate specificity unique to CueO originates in the methionine-rich helical region covering the substrate-binding site (5-7). Nevertheless, CueO has the same catalytic Cu centers as other multicopper oxidases: a type I Cu which mediates electron transfer, and a trinuclear Cu center comprised of a type II Cu and a pair of type III Cu atoms, where dioxygen is reduced to two water molecules (5,7). The type I Cu is responsible for the intense charge transfer band at 610 nm due to $Cys(S^-)_\pi \rightarrow Cu^{2+}$ and the bands at 430, ca. 500 and ca. 750 nm due to the charge transfers, $His(N) \rightarrow Cu^{2+}$ and $Cys(S^-)_\sigma \rightarrow Cu^{2+}$, and d-d transitions, respectively (4). The type III Cu atoms bridged with a hydroxide ion afford an intense charge transfer band, $OH^- \rightarrow Cu^{2+}$ at ca. 330 nm, while the type II Cu does not give a conspicuous band in the visible region. The type I Cu and type II Cu give rise to electron paramagnetic resonance (EPR) signals with the hyperfine splitting of small (6.7 mT) and normal (18.5 mT) magnitudes, respectively, while the type III Cu atoms are EPR-silent because of the strong antiferromagnetic interaction (7-9).

Special attention has been paid to the four-electron reduction of dioxygen by multicopper oxidases and terminal oxidases, since activated oxygen species such as superoxide, peroxide, etc. are not formed, or if formed are effectively converted into water molecules without damage to protein molecules. Therefore, this four-electron reduction of dioxygen by multicopper oxidases has been expected to be applicable to biofuel cells (10-12). Two reaction intermediates have been detected during reactions of some multicopper oxidases. One of them, the intermediate I, could be trapped by the following modified multicopper oxidases so as to interrupt the electron transfer from the type I Cu: a plant laccase whose type I Cu was substituted with Hg (13), a mixed valent laccase in which the type I Cu was oxidized but the trinuclear Cu center was reduced (14), and a Cys → Ser mutant of bilirubin oxidase (15) and Fet3p (16) whose type I Cu center became vacant. Although the trinuclear Cu center must be fully reduced to produce the intermediate I, it has been considered to be a two-electron reduced form, and, therefore, also called the peroxide intermediate (13,16). Another reaction intermediate, II, also called the native intermediate, has been detected at the final stage of a single turnover (15,17-19). Four electrons have already been transferred to dioxygen in this intermediate, and accordingly, the intermediate II is in a fully oxidized form to give the $g < 2$ EPR-signal at cryogenic temperatures. Under catalytic conditions the intermediate II is not detected because of its prompt

conversion to the fully reduced form for the next enzyme cycle without decaying to the resting form. Both intermediates have a half-life in the order of sec to min, but information to directly show their structures has not been obtained yet. They afford analogous absorption bands at ca. 330-350, 450-470, and 680 nm, of which the former two bands have been assigned to the charge transfer from a certain O group to Cu(II) (σ and π transitions) and the latter to the d-d transitions of the trinuclear Cu center in the cupric state. The d-d transitions of the intermediate II are masked by strong absorption due to the oxidized type I Cu (13-19).

In the present study, we succeeded in trapping the intermediates I and II from reactions of a recombinant form of CueO (rCueO) and mutants altered at Ser500, a ligand to the type I Cu, and at Asp112 and Glu506 located adjacent to the trinuclear Cu center, to modify the dioxygen reduction process. The Asp residue is conserved in every multicopper oxidase except for ceruloplasmin, which has Glu instead (Figure 1). According to the X-ray crystal structures of rCueO (5) and the truncated mutant, $\Delta\alpha$5-7CueO, missing the fifty amino acids covering the substrate-binding site (7,20) (Figure 2), Asp112 forms a hydrogen-bond with His448, a ligand to a type III Cu, and indirectly with the water molecule coordinating the type II Cu through an ordered water molecule. In a preliminary study on the Asp112 mutants (21), we showed that this acidic amino acid functions in the binding of dioxygen at the trinuclear Cu center, and may also be involved in the donation of protons to the reaction intermediate(s). On the other hand, one to three acidic amino acids are present in the spacers to connect the Cu ligands of multicopper oxidases, His-Cys-His-X-X-X-His-X-X-X-X-Met(Leu, Phe). Figure 2 shows that Glu506 of CueO in this spacer is directly hydrogen-bonded with the His143 ligand to one of the type III Cu atoms and indirectly with the hydroxide ion bridged between the type III Cu atoms through an ordered water molecule. Therefore, Glu506 is also speculated to play a crucial role in the reduction of dioxygen. We singly and doubly mutated Cys500, Asp112, and Glu506 of CueO in order to trap the intermediates I and II and to elucidate the mechanism behind the four-electron reduction of dioxygen.

EXPERIMENTAL PROCEDURES

Mutagenesis, Expression, and Purification—The genes for Cys500Ser, Asp112Asn, Glu506Gln, Cys500Ser/Asp112Asn, and Cys500Ser/Glu506Gln were synthesized with a QuickChange kit (Stratagene) using the oligonucleotide primers listed below and the template plasmid pUCCueO' as described in reference 12. The gene fragment encoding $\Delta\alpha$5-7CueO Cys500Ser was synthesized using the C500S primers and pUCCueO $\Delta\alpha$5-7 (7) as a template.

C500S(+), 5'-TATATGGCGCACTCCCATCTGCTG-3';
C500S(-), 5'-CAGCAGATGCGAGTGCGCCATATA-3';
D112N(+), 5'-CCGGGTGAAGTCAACGGCFGCC-3';
D112N(-), 5'-CTGCGGGCCGCCGTTGACTTCACC-3';
E506Q(+), 5'-CTGGAGCATCAAGATACGGGG-3';
E506Q(-), 5'-CCCCGTATCTTGATGCTCCAG -3'.

E. coli Origami (DE3)/pLacI (Novagen) was transformed with the mutant plasmids. Cultivation of the transformants and purification of the mutant proteins were carried out as described previously (7,20). Protein concentrations were determined using the BCA protein assay reagent (Pierce) and the absorption intensity at 280 nm ($\varepsilon = 73000$).

Enzyme Activities—Activities of the mutants for oxidizing ABTS, which functioned simply as an electron donor, were colorimetrically determined from the changes in absorption of the oxidized product of ABTS at 420 nm ($\varepsilon = 36000\ M^{-1}\ cm^{-1}$) in acetate buffer, pH 5.5 (3,7,20,21) (see the caption to Supplemental Figure 2). One unit of activity was defined as the amount of enzyme that oxidized 1 μmol of ABTS per minute.

Reactions—Reactions of rCueO and mutants with dioxygen were performed using a 5-mm path-length quartz cell with a long neck capped with a rubber septum to introduce dithionite through a thin needle under Ar. It took one night to fully reduce the single and double mutants with an altered Cys500 residue. After rCueO and mutants were fully reduced and no absorption at 314 nm due to the residual dithionite was observed, pure dioxygen gas was bubbled into the reaction mixture, and measurements of absorption spectra were started. In measurements of resonance Raman spectra, $^{18}O_2$ (Isotec 99%) was also used. The sample for EPR measurements was withdrawn from the reaction mixture with a syringe and frozen with liquid nitrogen. The total amount of EPR-detectable Cu^{2+} was determined by the double integration method using Cu-EDTA as a standard. Signal intensities due to the differences in tuning conditions were calibrated using a Mn^{2+} marker (JEOL) as an external standard. The reactions were performed at least twice to ascertain reproducibility.

Measurements—The total copper content of a protein molecule was determined by atomic absorption spectroscopy on a Varian SpectrAA-50 spectrometer. Absorption spectra were measured on a JASCO V-560 spectrometer and a Shimadzu Multispec-1500 spectrometer with a diode-allay detector for kinetic measurements. Circular dichroism (CD) spectra were measured on a JASCO J-500C spectropolarimeter. X-band EPR spectra were measured on a JEOL JES-RE1X spectrometer attached to an Oxford cryostat ESR900 between 77 K and 3.5 K. Resonance Raman scattering was excited at 488 nm with an Ar^+ laser (Spectra Physics, 2017) and detected with a CCD (Princeton Instruments) attached to a triple polychrometer (JACSO, NRS-1800). Fourier-transform infrared

(FT-IR) spectra were measured using a 0.025-mm path length ZnSe cell on a JASCO FT/IR-4200 spectrometer.

RESULTS

Cys500Ser

CueO lost exactly one Cu ion with the mutation of Cys500 to Ser, and did not show catalytic activity. Cys500Ser was colorless because the strong charge transfer band, $Cys(S^-) \rightarrow Cu^{2+}$ at 610 nm, was absent due to the loss of the type I Cu (absorption spectra of Cys500Ser (blue line) and rCueO (black line) in Figure 3A). On the other hand, a strong band derived from the $OH^- \rightarrow Cu^{2+}$ charge transfer was observed at 320 nm (ε = 5200), a 10-nm shorter wavelength from that of rCueO, indicating that the electronic state of the trinuclear Cu center was slightly affected due to the absence of the type I Cu at the remote site. The d-d transition band due to the type II Cu and type III Cu atoms, which had been masked by the intense d-d band of the type I Cu at ca. 750 nm (ε = 2000) in rCueO, became observable at ca. 710 nm (ε = ca. 500). The CD spectrum of Cys500Ser (blue line in Figure 3B) afforded bands at 323 ($\Delta\varepsilon$ = -2.6), 374 ($\Delta\varepsilon$ = +0.3), 504 ($\Delta\varepsilon$ = +0.8), 602 ($\Delta\varepsilon$ = -0.5), 698 ($\Delta\varepsilon$ = +0.5), and ca. 890 nm ($\Delta\varepsilon$ = -1.0) (The spectrum at 800-1000 nm is not shown). The CD bands were similar in number and intensity to those of the corresponding Cys $\rightarrow$ Ser mutant of bilirubin oxidase (15) and Fet3p (16), although some of them were inverted in sign. The EPR spectrum afforded only the signal due to the type II Cu (g_{II} = 2.24, $g_{\perp}$ = 2.04, A_{II} = 17.8 mT) with the five superhyperfine splittings originating from the coordination of the two His residues (A_N = 1.7 mT) at around 318 mT (blue line in Figure 3C). The total EPR detectable type II Cu(II) was 1.0 per protein molecule. The type III Cu atoms were EPR-silent as in rCueO.

It took almost one day to reduce Cys500Ser with a slight excess of dithionite under anaerobic conditions. This unusually slow reduction of the trinuclear Cu center, as was also observed in the case of the bilirubin oxidase mutant (15), originated from the absence of the type I Cu to mediate the electron-transfer between the substrate and the trinuclear Cu center. Soon after the start of the reaction of the reduced Cys500Ser with dioxygen, the transient spectrum coming from a reaction intermediate was obtained. Subtraction of the absorption spectrum of the reduced Cys500Ser afforded bands at 340 (ε = 9000), 470, and 680 nm, which were assigned to the $O^-_{\sigma} \rightarrow Cu^{2+}$ charge transfer, $O^-_{\pi} \rightarrow Cu^{2+}$ charge transfer, and d-d transitions, respectively (blue line in Figure 4A) based on similarities to those of the intermediate I derived from plant laccase, bilirubin oxidase, and Fet3p derivatives (14-16). The lifetime of the trapped intermediate I was very long even at room temperature (blue

squares in the inset in Figure 4A for the initial 8% decay showing a biphasic process with the half-life, $t_{1/2}$ = 320 min, in the second phase starting at ca. 10 min) and the absorption spectrum finally returned to that of the form isolated after one day (not shown). Owing to the long lifetime, we could observe the CD spectrum of the intermediate I (Figure 4B), which is very similar to that of Cys500Ser/Glu506Gln as isolated (green line in Figure 3B, *vide infra*). EPR spectra measured at between 77 and 3.5 K indicated that the intermediate I was EPR-silent (blue line in Figure 4C at 3.5 K). The signal intensity of the type II Cu was ca. 0.1 per protein molecule at the start of the reaction (1.0 Cu^{2+} before the reaction, dotted blue line in Figure 4C), and increased concomitantly with the decay of the intermediate I. A clear dependence on pH was not observed in the decay of the intermediate I, differing from the derivatives of laccase, bilirubin oxidase and Fet3p to suggest the participation of an acidic amino acid residue as a proton donor (14-16). The intermediate I could be obtained again using the recovered Cys500Ser, indicating that the trinuclear Cu center was not fatally damaged even after a prolonged period in the state of the intermediate I.

Cys500Ser/Asp112Asn

Cys500Ser/Asp112Asn also contained three Cu ions per protein molecule within an experimental error of 10%, and did not show any catalytic activity similarly to Cys500Ser. Cys500Ser/Asp112Asn also lacked absorption bands derived from the type I Cu (red line in Figure 3A). A strong band due to the $OH^- \rightarrow Cu^{2+}$ charge transfer characteristic of the resting trinuclear Cu center was observed at 315 nm (ε = 4800), 15 and 5 nm shorter than that of rCueO and Cys500Ser, respectively. The d-d transition band was observed at ca. 720 nm (ε = ca. 500). The CD spectrum of Cys500Ser/Asp112Asn (red line in Figure 3B) afforded bands at 317 ($\Delta\varepsilon$ = -2.2), ca. 380 ($\Delta\varepsilon$ = -0.5), 507 ($\Delta\varepsilon$ = +0.1), 600 ($\Delta\varepsilon$ = -0.7), 690 ($\Delta\varepsilon$ = +1.2), and ca. 880 nm ($\Delta\varepsilon$ = -1.2), (The spectrum at 800-1000 nm is not shown). The EPR spectrum (red line in Figure 3C) showed only the signal due to the type II Cu (g_{II} = 2.24, $g_{\perp}$ = 2.04, A_{II} = 17.8 mT) with five-superhyperfine splittings (A_N = 1.7 mT) at around 318 mT as in Cys500Ser. The total number of EPR-detectable type II Cu atoms was 1.0 per protein molecule, ensuring that the type III Cu atoms were EPR-silent.

The anaerobic reduction of Cys500Ser/Asp112Asn with a slight excess of dithionite was also very slow, similar to that of Cys500Ser. The formation of the intermediate I was, unlike in the case of Cys500Ser, very slow in spite of the continuous bubbling of pure O_2 into the reduced Cys500Ser/Asp112Asn solution. It took ca. 3 min for maximum formation of the intermediate I, which was only ca. 20% compared to the case of Cys500Ser (red line in Figure 4A). The bands derived from the intermediate I began to decrease with a half-life of $t_{1/2}$ = 99 min (red squares in the inset in Figure 4A) in spite of expectations that the intermediate I would be stabilized by introducing the mutation at

Asp112. EPR spectra observed between 77 and 3.5 K also indicated that the intermediate I was EPR-silent (red line in Figure 4C). The absorptions in the near UV regions began to increase very slowly after ca. 3hr, and finally gave an absorption spectrum similar to that of the form isolated after one day (not shown), suggesting that auto-oxidation of the reduced Cys500Ser/Asp112Asn took place.

rCueO

The reaction of rCueO was performed to detect the intermediate II. In contrast to Cys500Ser and Cys500Ser/Asp112Asn, rCueO was immediately reduced with the four-electron equivalent of dithionite. The absorption spectrum obtained soon after starting the reaction of the reduced rCueO with dioxygen was already analogous with that of the resting rCueO except for slightly higher absorption intensities at 300-500 nm. The lifetime of the intermediate II was too short to obtain an absorption spectrum, although the difference spectrum between the transient spectra (not shown) was similar to that obtained from the reaction of Glu506Gln (Figure 5A, *vide infra*) with much lower intensities. The EPR spectrum of the sample frozen within 5 sec after starting the reaction (black line in Figure 5C) gave a very broad signal with a trough, g = 1.85, at < 40 K in addition to the type I and type II Cu signals. The intensity of this novel EPR signal increased as the temperature dropped, indicating a rapid relaxation. Further, the increase in signal intensity was proportional to the square-root of microwave power at 3.5 K (black squares in Supplemental Figure 1 in the range of 1 to 100mW) in contrast to the type I and type II Cu signals, which began to saturate at < 1mW. Therefore, it is apparent that the novel EPR signal originated not from an isolated species but from a coupled species magnetically. This g = 1.85 EPR signal disappeared after the sample was thawed and frozen again, indicating that it was derived from the intermediate II.

Glu506Gln

Glu506Gln contained four Cu ions per protein molecule as determined by atomic absorption spectroscopy, and afforded absorption, CD and EPR (type I Cu: g_{II} = 2.24, $g_{\perp}$ = 2.04, A_{II} = 6.3 mT), type II Cu: g_{II} = 2.24, $g_{\perp}$ = 2.04, A_{II} = 17.3 mT) spectra similar to those of rCueO except for a blue shift by 5 nm and a slight decrease in the intensity of the charge transfer band, $OH^- \rightarrow Cu^{2+}$ (purple line in Figure 3). However, the catalytic activity shown by Glu506Gln was extremely low (V_{max} = 0.0041 units/mg, Supplemental Figure 2) compared to those of rCueO (V_{max} = 1.1 units/mg for rCueO) (7,21). Glu506Gln was reduced with a slight excess of dithionite as rapidly as rCueO, and gave the intermediate II soon after the start of the reaction with dioxygen (Supplemental Figure 1B). Subtraction of the reduced Gln506Gln spectrum gave the absorption spectrum of the intermediate II

with absorption maxima at 310 and 350 nm (ε = 4200) and a shoulder at ca. 410 nm (purple line in Figure 5A). The electron transfer from the type I Cu to dioxygen has already finished as is evident from the full recovery of absorption at 610 nm. The absorptions at 350 nm exponentially decayed with $t_{1/2}$ = 64 min (inset in Figure 5A), and the spectrum returned to that of the original Glu506Gln after one day. The CD spectrum between 300 and 500 nm measured within 5 min after the start of the reaction (purple line in Figure 5B), gave a negative band at 332 nm, which was red-shifted by 12 nm from that of Glu506Gln (dotted purple line). The EPR spectrum at 3.5 K (purple line in Figure 5C) gave a clear trough at g = 1.94, which was not saturated with increasing microwave power (purple squares in Supplemental Figure 1A in the range of 1 to 100 mW). On subtraction of the type I Cu signal, the presence of the g = 2.12 component became evident (inset in Figure 4C) as has been reported in a laccase study (27). Except for this novel signal observable at below 40 K, only the type I Cu EPR signal was observed. The type II Cu signal became observable with the disappearance of the g = 1.94 signal (spectra not shown).

Cys500Ser/Glu506Gln

Cys500Ser/Glu506Gln contained three Cu ions per protein molecule as determined by atomic absorption spectroscopy, and did not show enzyme activities. The absorption spectrum of Cys500Ser/Glu506Gln (green line in Figure 3A) was quite different from that of Cys500Ser or Cys500Ser/Asp112Asn, showing bands at 330 (ε = 7000), 480, and 680 nm, which are characteristic of the intermediate I (Figure 4A). The CD spectral features (Figure 3B) were also practically the same as those of the intermediate I (Figure 4B). Therefore, it is apparent that the state of the reaction intermediate I is realized in the resting Cys500Ser/Glu506. Although the type II Cu signal was observed in the EPR spectrum (Figure 4C), its intensity was $0.37Cu^{2+}$ ions per protein molecule. Therefore, the residual ca. 2/3 type II Cu ions were in the EPR–undetectable Cu^{+} state. Analogous spectral features were obtained in the Cys500Ser mutant of the Δα5-7CueO, in which the 50 amino acids covering the substrate-binding site were removed from the rCueO molecule, showing only the 0.1 type II Cu EPR signal (g_{II} = 2.24, $g_{\perp}$ = 2.04, A_{II} =18.3 mT) (Supplemental Figure 3).

DISCUSSION

Effects of Mutations at Asp112, Cys500, and Glu506 on the Electronic State of the Trinuclear Cu Center

The electronic state of the trinuclear Cu center was slightly modified by the mutations at Cys500, Asp112, and Glu506 as reflected in the blue-shift of the $OH^- \rightarrow Cu^{2+}$ charge transfer band: ca. 10 nm in Cys500Ser, ca. 15 nm in Cys500Ser/Asp112, and ca. 5 nm in Glu506Gln. These shifts in the 330 nm band presumably became observable because of the much low absorption intensity of the 280 nm band in CueO (ε = 73000) compared to other multicopper oxidases, for example, ε = 120000 in bilirubin oxidase (15). The modifications induced by the absence of a type I Cu were due to the type I Cu center and the trinuclear Cu center being connected with the His-Cys-His sequence and a peptide backbone in spite of their separation by ca. 13 Å (Figures 1 and 2) (5-7). On the other hand, modifications induced by the mutations at Asp112 and Glu506 were derived from the breaking down of the hydrogen bonds with a His ligand to a type III Cu and the coordinated water molecule to the type II Cu or the coordinated hydroxide ion between type III Cu atoms through a water molecule. These modifications at the remote type I Cu site and the non-coordinating Asp112 and Glu506 were mild as reflected in the absorption, CD and EPR spectra (Figure 3), but prominent enough to allow us to trap the intermediates I and II by shutting down the steps to supply electron or proton and by affecting the affinity of the trinuclear Cu center for dioxygen (*vide infra*).

In contrast to the above mutants, Cys500Ser/Glu506Gln (Figure 3) and the Cys500Ser mutant of Δα5-7CueO as isolated (Supplemental Figure 3) gave absorption, CD, and EPR spectra typical of the intermediate I (Figure 4). The classical definition of a resting trinuclear Cu center is that the type III Cu atoms are antiferromagnetically coupled with a bridged hydroxide ion and the type II Cu is magnetically isolated. However, trinuclear Cu centers in an exceptional state have been discovered by analyzing X-ray crystal structures of fungal laccases (22,23) and CotA (24), and with improvements in resolution of the X-ray crystallography of human ceruloplasmin (25): dioxygen or a reaction intermediate is located between type III Cu atoms in a side-on fashion or an oxygen atom is asymmetrically positioned near one of the type III Cu atoms. These modes of binding of dioxygen might involve that in the intermediate I, and it may not necessarily be unusual that the intermediate I is the dominant resting form in Cys500Ser/Glu506Gln and the Cys500Ser mutant of Δα5-7CueO (*vide infra*), although further studies on these mutants are required.

Intermediate I

The intermediate I trapped by the reaction of Cys500Ser unequivocally showed absorption bands at 340, 470 and 680 nm. These spectral features are very similar to those produced by a Hg-substituted or mixed valent laccase (13,14), and Cys to Ser mutants of bilirubin oxidase (15) and Fet3p (16), indicating that multicopper oxidases commonly pass through the intermediate I. The intensity of the

intermediate I band was much higher at 340 nm (ε = 9000) than at 315-330 nm due to the resting trinuclear Cu center (ε = 4500-5300) (Figure 3A and 4A). This fact and small molecule studies (26) suggest that the origin of the O atom concerned in the charge transfer ($O \rightarrow Cu^{2+}$) of the intermediate I is not hydroxide but peroxide. The CD spectrum indicated that the absorption band at 340 nm is composed of two bands at 315 and 365 nm and accordingly, the two O atoms are not equivalent (26). Thus, the structure shown in Figure 6 is depicted by taking the fact that the intermediate I is EPR-silent into consideration. Dioxygen is bound as peroxide between type III Cu atoms in the μ-η^2:η^2-fashion as in oxy-hemocyanin (27), with an additional interaction with the reduced type I Cu. Other possible structures, in which an O atom of hydroperoxide ion is bridged between type III Cu atoms in an end-on fashion (28) and the five-centered structure comprised of $2Cu^{2+}1Cu^{3+}2O^{2-}$ (8), may be excluded given that the two O atoms are not equivalent. A three-electron reduced form might be also excluded because a radical species derived from a break of the O-O bond was not detected by cryogenic EPR measurements. We excited the Raman scattering of the intermediate I at 488nm, which was close to the maximum absorption wavelength of a new absorption band of the intermediate I. However, we observed no oxygen-isotope sensitive band in the region 500-1200 cm^{-1}, although fluorescence was not as strong as in bilirubin oxidase (spectra not shown, 15). The intermediate I was very sensitive to the laser light due to photoreduction of the metal site or photodissociation of the oxygenated species, and accordingly, we could not accumulate the Raman spectrum for a long time. FT-IR measurements did not give any band derived from the intermediate I either.

In the reaction of the single mutant, Asp112Asn, with dioxygen, a very slow recovery of the blue color was observed (data not shown). This is consistent with our previous finding that the K_m value for the binding of O_2 changed from 0.019 to 0.035 mM, and enzyme activities were reduced to ca. 2-10 % by the mutation (21). Therefore, it is apparent that Asp112 is involved not only in the binding of dioxygen by forming a hydrogen bond with His448 but also in the later steps of a catalytic cycle influencing in the overall activities of the enzyme. An analogous study on the Asp94Asn mutant of Fet3p (19,29) proposed that deprotonation from the water molecule coordinated to the cuprous type II Cu was assisted by the hydrogen bond involving Asp94, leading to the strong binding of the peroxide ion to the trinuclear Cu center, although the coordination of the hydroxide to the cuprous type II Cu has not been proved. The critical role of Asp112 is also reflected in the remarkably slow and partial formation of the intermediate I from the double mutant, Cys500Ser/Asp112Asn (Figure 4). Considering these essential roles of Asp112 in the formation of the intermediate I, the possibility that Asp112 directly interacts with the peroxide ion can not be excluded. One Gly residue is followed by this Asp residue according to the amino acid sequence of multicopper oxidases (Figure 1), affording a flexibility or space in this region. Further, an additional Gly residue is followed by this Asp-Gly sequence in CueO and a structural homologue of multicopper oxidase, SufI (FtsP), involved in cell

division (30).

Glu506 might also contribute to the binding of peroxide at the trinuclear Cu center by forming hydrogen bonds with His143 coordinated to a type III Cu and with the peroxide ion directly or indirectly through a water molecule (Figure 6). The carboxy group in the side chain of Glu506 and one of the O atoms in the peroxide ion are close enough to directly form a hydrogen bond, if the peroxide ion is bound between the type III Cu atoms in the μ-η^2:η^2-fashion (Figure 2). However, the first step, in which the reduced Glu506Gln reacts with O_2, was not inhibited (*vide infra*) in contrast to Asp112Asn, indicating that the major role of Glu506 is to donate a proton to the intermediate I and perhaps also to the intermediate II for their prompt decay (*vide infra*). The discovery of the very stable intermediate I state in the resting Cys500Ser/Glu506Gln (Figure 3) indirectly supports this, while supplies of electrons from the type I and type II Cu atoms are also required for the decay of the intermediate I.

The decay of the intermediate I did not show a clear dependence on pH presumably because it occurred very slowly without a supply of protons directly or indirectly from Glu506 and electron from the type I Cu. In the cases of laccase and Fet3p, the intermediate I decayed faster with decreasing pH, suggesting the involvement of an acidic amino acid with a pK_a value of 5.0-5.6 (14,16,28). In addition, the decay of the intermediate I did not involve the formation of the intermediate II. We added a small amount of dithionite to the intermediate I under Ar, expecting to observe its conversion to the intermediate II. However, there was no conversion because of the absence of the type I Cu to mediate the prompt transfer of electron. Nevertheless, the intermediate I reached the same state as Cys500Ser isolated after one day presumably due to an unknown autooxidation process. In the catalytic cycle of CueO, supplies of electrons from the type I Cu and type II Cu and protons from Glu506 will realize the prompt conversion of the intermediate I to the intermediate II, and this is why the intermediate I has not been detected during the reaction of CueO.

Intermediate II

In contrast to the intermediate I, all four Cu centers should be reduced to form the intermediate II. The absorption and EPR spectra clearly showed that the electron transfer from the type I Cu had finished in the intermediate II (Figure 5). However, the intermediate II formed from Glu506Gln did not show the type II Cu EPR signal (Figure 5C bottom), while the signal was observed in the reaction of rCueO (Figure 5C middle) probably because most of rCueO had already reached the resting state due to the rapid reaction of the unmodified enzyme. However, the intermediate II formed from Glu506Gln afforded a unique EPR signal (g = 2.12 and 1.94) detectable at < 40K, which increased in intensity as temperature decreased, and was not saturated with high-power microwaves (Supplemental

Figure 1A). Therefore, all Cu centers in the trinuclear Cu center are magnetically coupled (3Cu(II) system) and in a low-lying excited state (27). The difference in the parameters derived from laccase (g = 1.6 or 1.8) (18,28), rCueO (g = 1.85), and Glu506Gln (g = 1.94) suggests that the difference in the magnitude of the magnetic interaction is in the order, laccase > rCueO > Glu506Gln.

The intermediate II formed from Glu506Gln gave an absorption maximum at 315 nm (noticeable by subtracting the spectrum of the reduced Glu506Gln) and 350 nm (ε = 4200) and a shoulder at around 410 nm, while absorption between 500 and 800 nm was masked by the strong absorption derived from the oxidized type I Cu (Figure 5A). The absorption band at 350 nm was not as intense as those of the intermediate I. This strongly suggests that the O-O bond is cleaved as shown by the study of small binuclear-Cu molecules (26). In harmony with the shift in the absorption band from 325 nm to 350 nm, the corresponding CD band shifted from 318 ($\Delta\varepsilon$ = –2.0) nm to 332 nm ($\Delta\varepsilon$ = –2.1). The intermediate II disappeared after one day, and the absorption spectrum returned to that of Glu506Gln as isolated. The prominent slowing down in the decay of the intermediate II by the mutation at Glu506 ($t_{1/2}$ = 64 min) indicates that this amino acid plays a critical role in the supply of a proton to the intermediate II.

The structure shown in Figure 6 satisfies the properties of the intermediate II: the presence of the charge transfer band $O^{2-} \rightarrow Cu^{2+}$ which was red-shifted and reduced in intensity compared to that from the intermediate I, the presence of the reoxidized type I Cu, the absence of the type II Cu EPR signal, and production of the g < 2 EPR signal. Another isoelectronic form might be that an O-centered radical is bound to the cuprous type II Cu (18) or the radical center is delocalized between an O atom and the type II Cu. These structures have been excluded in laccase and Fet3p studies (19,28,29), while no direct evidence is available yet.

The present detection of the intermediate II and characterizations are due to the mutation at Glu506, indicating that the role of this amino acid is to donate a proton to the intermediate II for its prompt decay. We did not study the temperature-dependence of the decay process due to the very long lifetime of the intermediate II, and accordingly we could not ascertain whether a large change takes place in the framework of the trinuclear Cu center during the conversion of the intermediate II to the resting form (18, 31). The location of the amino acid corresponding to Glu506 in CueO, Glu510 in ascorbate oxidase (32), Glu499 or Glu504 in plant laccase (33), Glu487 in Fet3p (19), and Glu498 in CotA (24), is not rigorously conserved in the amino acid sequence of multicopper oxidase, (Figure 1). However, all these Glu residues form a hydrogen bond with a His ligand to a type III Cu as indicated in the 3D structures (32,34,35) with the exception of Asp1025 in ceruloplasmin (25).

Conclusions

In summary, the four-electron reduction of dioxygen by CueO is accomplished in two two-electron steps through the intermediates I and II. The binding of dioxygen to the trinuclear Cu is independent of the presence of the type I Cu, and reaches the intermediate I with the assistance of the reduced type II Cu and Asp112, although the involvement of this intermediate in the catalytic process has not been proved. In the second two-electron transfer step, the type I Cu and type II Cu function as electron donors and Glu506 assists the transfer of a proton to the intermediate I. Conversion of the intermediate II to the resting form is markedly slowed by the mutation at Glu506, indicating the direct or indirect assistance of Glu506 to donate a proton to the intermediate II. In the catalytic cycle, the intermediate II may be promptly reduced for the next cycle without reaching the resting form. Thus, the present study on the intermediates I and II of CueO unequivocally shows that the assistance of Asp112 and Glu506 located at the "outersphere" of the trinuclear Cu center is indispensable in the four-electron reduction of dioxygen by CueO. A different mechanism, whereby dioxygen is captured between type III Cu atoms in the resting form, has been proposed for CotA (35), although two intermediates corresponding to I and II are also suggested.

REFERENCES

1. Outten, F. W., Huffman, D. L., Halem J. A., and O'Halloran, T. V. (2001) *J. Biol. Chem.* **276**, 30670-30677
2. Rensing, C. and Grass, G. (2003) *FEMS Microbiol. Rev.* **27**, 197-213
3. Grass, G., Thakali, K., Klebba, P. E., Thieme, D., Muller, A., Wilder, G. F., and Rensing, C. (2004) *J. Bacteriol.* **186**, 5826-5833
4. Messerschmidt, A. ed. (1997) *Multi-copper Oxidases*, World Scientific, Singapore
5. Roberts, S. A., Weichsel, A., Grass, G., Thakail, K., Hazzard, J. T., Tollin, G., Rensing, C., and Montfort, W. R. (2002) *Proc. Natl. Natl. Acad. Sci. U. S. A.* **99**, 2766-2771
6. Singh, S., Grass, G., Rensing, C., and Montfort, W. R. (2004) *J. Bacteriol.* **186**, 7815-7817
7. Kataoka, K., Komori, H., Ueki, Y., Konno, Y., Kamitaka, Y., Kurose, S., Tsujimura, S., Higuchi, Y., Kano, K., and Sakurai, T. (2007) *J. Mol. Biol.* **373**, 141-152
8. Sakurai, T. and Kataoka, K. (2007) *Chem. Rec.* **7**, 220-229
9. Sakurai, T. and Kataoka, K. (2007) *Cell. Mol. Life Sci.* **64**, 2642-2656
10. Miura, Y., Tsujimura, S., Kamitaka, Y., Kurose, S., Kataoka, K., Sakurai, T., and Kano, K. (2007) *Chem. Lett.* **36**, 132-133
11. Tsujimura, S., Miura, Y., and Kano, K. (2008) *Electrochim. Acta* **53**, 5716-5720
12. Miura, Y., Tsujimura, S., Kurose, S., Kataoka, K., Sakurai, T., and Kano, K. (2009) *Fuel Cells* **9**, 70-78
13. Shin, W., Sundaram, U. M., Cole, J. L., Zhang, H. H., Hedman, B., Hodgson, K. O., and Solomon, E. I. (1996) *J. Am. Chem. Soc.* **118**, 3202-3215
14. Zoppellaro, G., Sakurai, T., and Huang, H.-W. (2001) *J. Biochem.* **129**, 949-953
15. Kataoka, K., Kitagawa, R., Inoue, M., Naruse, D., Sakurai, T., and Huang, H.-W. (2005) *Biochemistry* **44**, 7004-7012
16. Palmar, A. E., Quintanar, L., Severance, S., Wang, T., Kosman, D. J., and Solomon, E. I. (2002) *Biochemistry* **41**, 6438-6448
17. Lee, S., George, S. D., Antholine, W. E., Hedman, B., Hodgson, K. O., and Solomon, E. I. (2002) *J. Am. Chem. Soc.* **124**, 6180-6193
18. Huang, H.-W., Zoppellaro, G., and Sakurai, T. (1999) *J. Biol. Chem.* **274**, 32718-32724
19. Augustine, A., Quintanar, L., Stoj, C. S., Kosman, D. J., and Solomon, E. I. (2007) *J. Am. Chem. Soc.* **129**, 13118-13126
20. Kurose, S., Kataoka, K., Otsuka, K., Tsujino, Y., and Sakurai, T. (2007) *Chem. Lett.* **36**, 232-233
21. Ueki, Y., Inoue, M., Kurose, S., Kataoka, K., and Sakurai, T. (2006) *FEBS Lett.* **580**, 4069-4072
22. Hakulinen, N., Kruus, K., Koivula, A, and Rouvinen, J. (2006) *Biochim, Biophys. Res. Commun.*

350, 929-934

23. Garvaglia, S., Cambria, M, T., Miglio, M., Ragusa, S., Lacobazzi, V., Palmieri, F., D'Ambrosio, C., Scaloni, A., Rizzi, M. (2004) *J. Mol. Biol*. **342**, 1519-1531
24. Durao, P., Bento, I., Fernandes, T., Melo, E. P., Lindley, P. F., and Martins, L. O. (2006) *J. Biol. Inorg. Chem.* **11**, 514-526
25. Bento I., Zaitzev, V. N., and Lindley, P. F. (2007) *Acta Cryst.* **D63**, 240-248
26. Lewis, E. A. and Tolman, W. B. (2004) *Chem Rev*. **104**, 1047-1076
27. Magnus, K. A., Hazes, B., Ton-That., H., Bonaventura, C., Bonaventura, J., and Hol. W. G. (1994) *Proteins*, **19**, 302-309
28. Solomon, E. I., Chen, P., Metz, M., Lee, S., and Palmer A. E. (2001) *Angew. Chem.* **40**, 4570-4590
29. Quintanar, L., Stoj, C., Wang, T., Kosman, D. J., and Solomon, E. I, (2005) *Biochemistry* **44**, 6081-6091
30. Kato, J., Nishimura, Y., Yamada, M., Suzuki, H., and Hirota, Y. (1988) *J. Bacteriol.* **170**, 3967-3977
31. Yoon, J. and Solomon, E. I. (2007) *J. Am. Chem. Soc.* **129**, 13127-13136
32. Messerschmidt, A., Ladenstein, R., Huber, R., Bolognesi, M., Avigliano, L., Petrusselli, R., Posi, A., and Finazzi-Agro, A. (1992) *J. Mol. Biol*. **224**, 179-205.
33. Nitta, K., Kataoka, K., and Sakurai, T. (2002) *J. Inorg. Biochem*. **91**, 125-131.
34. Taylor, A. B., Stoj, C. S., Ziegler, L., Kosman, D. J. and Hart, P. J. (2005) Proc. Natl. Acad. Sci. 102, 15459-15464.
35. Bento, I., Martins, L. O., Lopes, G. G., Carrondo, M. A., and Lindley, P. F. (2005) *Dalton Trans.*, 3507-3513

Footnote

*This work was supported by a Grant-in-aid for Scientific Research from the Ministry of Education, Culture, Sports, Science and Technology of Japan (19350081 to T.S.) and by NEDO. The authors also thank Mandom Corporation and Toyota Motor Corporation for financial support and Kyoto Advanced nanotechnology Network for the resonance Raman measurements.

[1]The abbreviations used are: CueO, Cu efflux oxidase; BCA, bicinchoninic acid; ABTS, 2,2'-azino-bis(3-ethylbenzothiazoline-6-sulfonic acid; rCueO, recombinant CueO; EPR, electron paramagnetic resonance; EDTA, *N*,*N*,*N*',*N*'-ethylenediaminetetraacetic acid: CD, circular dichroism; FT-IR, Fourier transform infrared.

Figure Captions

FIGURE 1. **Homology of amino acid sequence around the Cu binding sites of multicopper oxidase.** The numbers, 1, 2, and 3 represent the type I Cu, type II Cu, and type III Cu ligand, respectively. BO, *Myrothecium verrucaria* bilirubin oxidase; RvLc, *Rhus vernicifera* laccase; CpAO, *Cucurbita pepo* ascorbate oxidase; TvLc, *Trametes versicolor* laccase; CcLc, *Coprinus cinerius* laccase; Fet3p, multicopper oxidase from *Saccharomyces cerevisiae;* CumA, multicopper oxidase from *Pseudomonas putida*; CotA, multicopper oxidase from *Bacillus subtilis*; SLAC, small laccase from *Streptomyces coelicolor*; hCp, human ceruloplasmin. The single asterisk represents the conserved acidic amino acid residue in all multicopper oxidases, and the double asterisk represents Glu506 in CueO which forms a hydrogen bond with a His residue coordinating a type III Cu and the hydroxide ion bridged between type III Cus.

FIGURE 2. **Structure around the active site of the truncated mutant of CueO** (7). Type I, II, and III Cus are represented as spheres. Small spheres are oxygen atoms. The two networks of hydrogen bonds lead to the exterior of the protein molecule, forming the pathway to let protons in and water molecules out. Mutated amino acid residues, Cys500, Glu506 and Asp112, and the networks of hydrogen bonds are indicated.

FIGURE 3. **Absorption (A), CD (B) and EPR (C) spectra of rCueO (black) and mutants, Cys500Ser (blue), Cys500Ser/Asp112Asn (red), Glu506Gln (purple), and Cys500Ser/Glu506Gln (green).** Absorption and CD spectra of ca. 100 μM proteins in 0.1 M phosphate buffer, pH 7 were measured at room temperature using an 1 cm path-length quartz cell. The units of the ordinate are based on the protein molecule. EPR spectra were measured at 77K, frequency 9.2 GHz, microwave power 4 mW, modulation 1 mT at 100 kHz, filter 0.3 s, sweep time 4 or 8 min, and amplitude 200-400. The EPR spectra are normalized to give analogous signal intensities except for Cys500Ser/Glu506Gln. The total numbers of the EPR-detectable Cu^{2+} in rCueO, Cys500Ser, Cys500Ser/Asp112Asn, Glu506Gln, and Cys500Ser/Glu506Gln are 2.0, 1.0, 1.0, 1.0, and 0.36 per protein molecule, respectively.

FIGURE 4. **Absorption (A), CD (B), and EPR (C) spectra of the intermediate I derived from Cys500Ser (blue) and Cys500Ser/Asp112Asn (red).** The inset in Figure 4A shows the absorbance decay of the intermediate I at 340 and 330nm formed from Cys500Ser and Cys500Ser/Asp112Asn, respectively. Sample conditions for measurements of absorption and CD spectra are the same as those in Figure 3 except that a 0.5-cm path-length cell was used for ca. 100-200 μM proteins. EPR spectra

were measured at 3.5 K, frequency 9.0 GHz, microwave power 1 mW, modulation 1 mT at 100 kHz, filter 0.3 s, sweep time 4 or 8 min, and amplitude 400. The spectrum of Cys500Ser before the reaction (dotted blue) is also shown for comparison.

FIGURE 5. **Absorption (A), CD (B), and EPR (C) spectra of the intermediate II derived from rCueO (black) and Glu506Gln (purple).** The absorption spectrum of the intermediate II formed from Glu506Gln (Figure 5A) was obtained from Supplementary Figure 1B. Sample conditions are the same as those for Figure 3. The inset in Figure 5A shows the absorbance decay of the intermediate II at 350 nm. The measurement of the CD spectrum at <500 nm (Figure 5B) was accomplished within 5 min after starting the reaction to avoid the masking effect due to the oxidized type I Cu. Figure 5C shows the EPR spectrum of rCueO (dotted black) and the spectra obtained soon after the reactions of rCueO (black) and Glu506Gln (purple) at 3.5 K, frequency 9.0 GHz, microwave power 1-100 or 200 mW, modulation 1 mT at 100 kHz, filter 0.3 s, sweep time 4 or 8 min, and amplitude 400-2000. The inset in Figure 5C shows the overall EPR signal of the intermediate II, which was obtained by subtracting the type I Cu signal.

FIGURE 6. **The Four-electron reduction of dioxygen by CueO.** The structure of the resting CueO is based on the X-ray crystal structure of rCueO (5) and the truncated mutants (7). It is not known whether water molecules are present near the active site in the reduced CueO. The most probable peroxide-bound structure for the intermediate I is figured to account for the production of the charge transfer bands due to $O_2^{2-} \rightarrow Cu^{2+}$ and to be EPR-silent. The intermediate I is converted into the intermediate II with the supply of electrons from type I Cu and type II Cu and of a proton with the assistance of Glu506. In the intermediate II, four electrons are transferred to dioxygen and the O-O bond is cleaved. Type II and III Cu's are magnetically interacted to give the $g < 2$ EPR signal. In the decay of the intermediate II, another proton is donated with the assistance of Glu506.

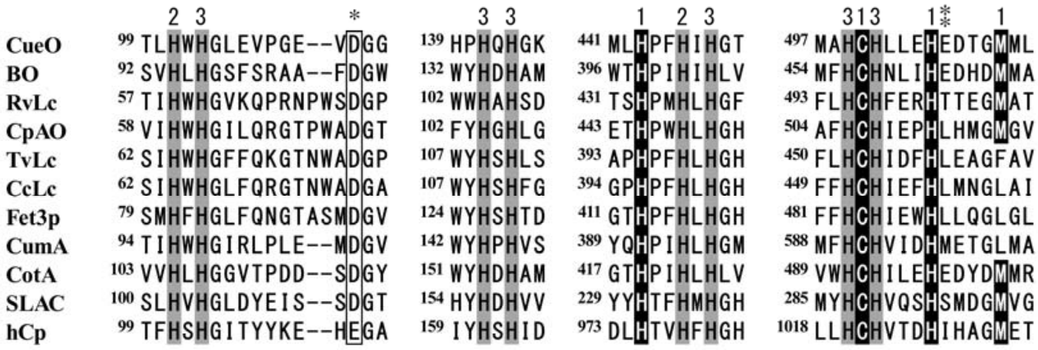
2 3
*
3 3
1 2 3
313
1
1
CueO 99 TLHWHGLEVPGE--VDGG 139 HPHQHGK 441 MLHPFHIHGT 497 MAHCHLLEHEDTGMML
BO 92 SVHLHGSFSRAA--FDGW 132 WYHDHAM 396 WTHPIHIHLV 454 MFHCHNLIHEDHDMMA
RvLc 57 TIHWHGVKQPRNPWSDGP 102 WWHAHSD 431 TSHPMHLHGF 493 FLHCHFERHTTEGMAT
CpAO 58 VIHWHGILQRGTPWADGT 102 FYHGHLG 443 ETHPWHLHGH 504 AFHCHIEPHLHMGMGV
TvLc 62 SIHWHGFFQKGTNWADGP 107 WYHSHLS 393 APHPFHLHGH 450 FLHCHIDFHLEAGFAV
CcLc 62 SIHWHGLFQRGTNWADGA 107 WYHSHFG 394 GPHPFHLHGH 449 FFHCHIEFHLMNGLAI
Fet3p 79 SMHFHGLFQNGTASMDGV 124 WYHSHTD 411 GTHPFHLHGH 481 FFHCHIEWHLLQGLGL
CumA 94 TIHWHGIRLPLE--MDGV 142 WYHPHVS 389 YQHPIHLHGM 588 MFHCHVIDHMETGLMA
CotA 103 VVHLHGGVTPDD--SDGY 151 WYHDHAM 417 GTHPIHLHLV 489 VWHCHILEHEDYDMMR
SLAC 100 SLHVHGLDYEIS--SDGT 154 HYHDHVV 229 YYHTFHMHGH 285 MYHCHVQSHSMDGMVG
hCp 99 TFHSHGITYYKE--HEGA 159 IYHSHID 973 DLHTVHFHGH 1018 LLHCHVTDHIHAGMET

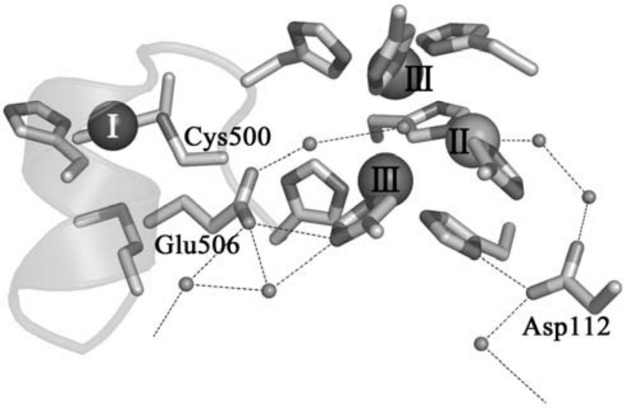
III
I
Cys500
II
III
Glu506
Asp112

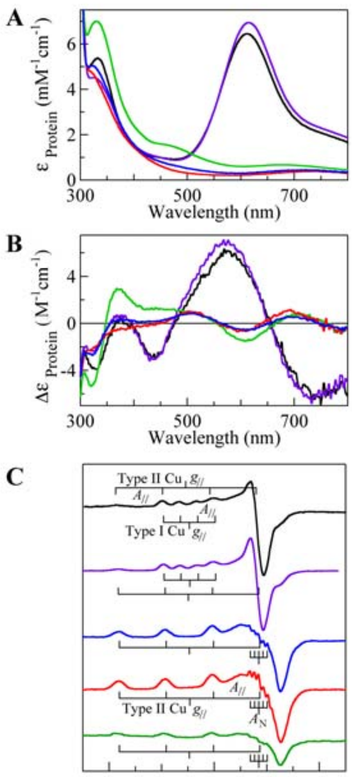
A
ε Protein (mM-1cm-1)
6
4
2
0
300
500
700
Wavelength (nm)
B
Δε Protein (M-1cm-1)
4
0
-4
300
500
700
Wavelength (nm)
C
Type II Cu
g//
A//
Type I Cu
g//
A//
A//
Type II Cu
g//
AN
260
300
340
Magnetic Field (mT)

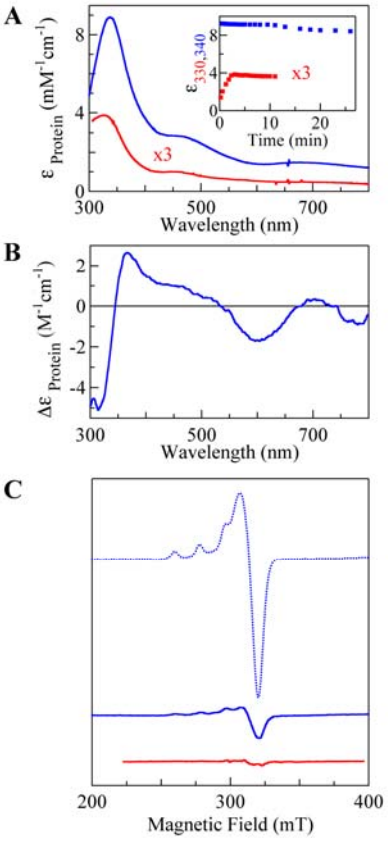
A
ε Protein (mM-1cm-1)
8
4
0
300
500
700
Wavelength (nm)
x3
ε330,340
8
4
0
0
10
20
Time (min)
x3
B
Δε Protein (M-1cm-1)
2
0
-2
-4
300
500
700
Wavelength (nm)
C
200
300
400
Magnetic Field (mT)

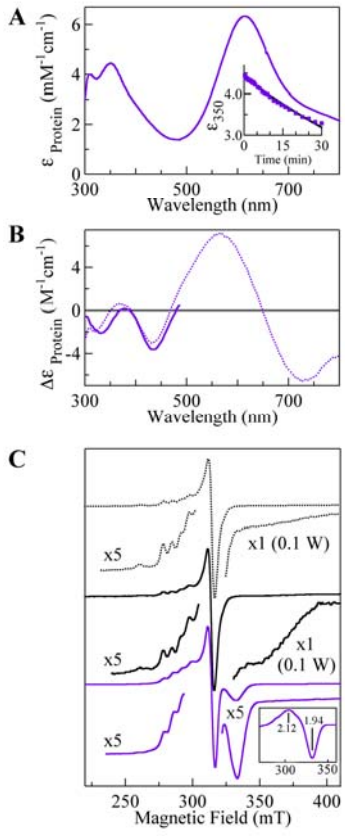
A
ε Protein (mM-1cm-1)
6
4
2
0
300
500
700
Wavelength (nm)
ε350
4.0
3.0
0
15
30
Time (min)
B
Δε Protein (M-1cm-1)
4
0
-4
300
500
700
Wavelength (nm)
C
x5
x1 (0.1 W)
x5
x1
(0.1 W)
x5
x5
2.12
1.94
300
350
250
300
350
400
Magnetic Field (mT)

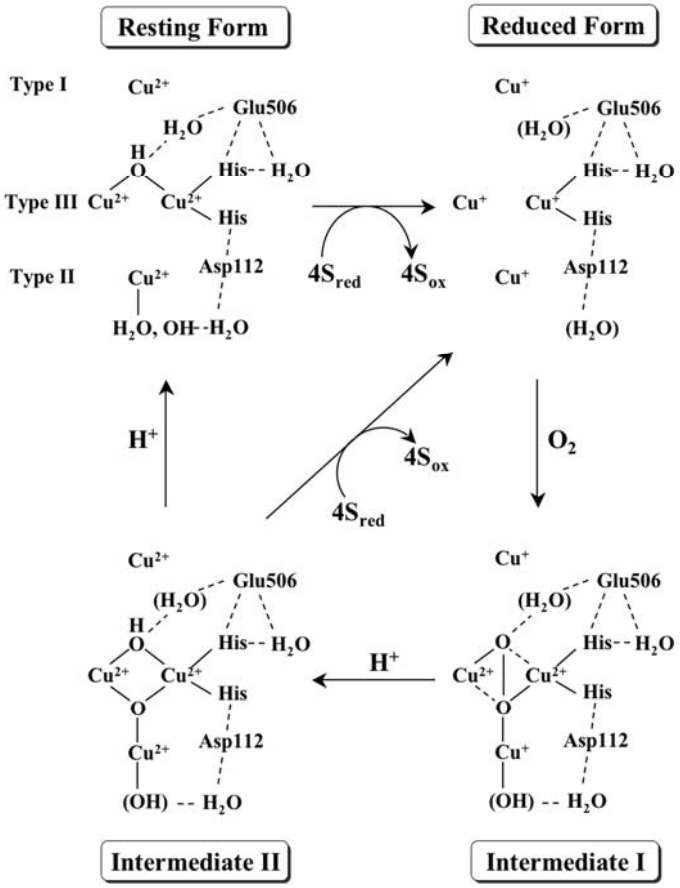
Resting Form
Reduced Form
Type I
Type III
Type II
Cu2+
Glu506
H2O
H
O
His
Cu+
Asp112
4Sred
4Sox
H+
O2
Intermediate II
Intermediate I
(H2O)
(OH)